ISSN 1505-4675

Technical Sciences

17(2) 2014

Biosystems Engineering
Civil Engineering
Environmental Engineering
Geodesy and Cartography
Information Technology
Mechanical Engineering
Production Engineering

Technical Sciences 17(2), 2014, 135–148

MODIFICATION OF THE PATHFINDER ALGORITHM FOR CALCULATING GRANULAR BEDS WITH VARIOUS PARTICLE SIZE DISTRIBUTIONS

Waldemar Dudda, Wojciech Sobieski

Department of Mechanics and Machine Design
University of Warmia and Mazury in Olsztyn

Received 19 May 2014, accepted 18 June 2014, available on line 18 June 2014

K e y w o r d s: PathFinder code, porous media, granular beds, tortuosity.

A b s t r a c t

This paper discusses a new approach to analyzing fluid flow through a granular bed. The analysis involves the determination of a set of geometric parameters characterizing a granular bed based on information about the location and diameter of all bed particles. The above task has been achieved with the use of the PathFinder numeric code developed by the authors. The study proposes a new algorithm for calculating the parameters of granular beds composed of spherical particles with various diameters in the PathFinder program. The algorithm has been verified with the use of independent tools and implemented in the new version of the PathFinder code. The modified algorithm's effect on flow path tortuosity has been analyzed. Path length is used to determine tortuosity, a key parameter of pore geometry that is difficult to calculate. Comparative calculations were performed in a granular bed generated by the Discrete Element Method in the PFC^{3D} program.

Introduction

Granular porous media comprising spherical or quasi-spherical particles play an important role in various technological and engineering processes. Due to the widespread occurrence of porous media, mathematical models describing the behavior of a granular medium, also known as a granular bed, or its interactions with the environment are of great practical significance. Models predicting resistance (pressure loss) during fluid flow through granular media have attracted particular interest. Despite many years of research, a satisfactory solution to the problem has not yet been proposed (SOBIESKI, TRYKOZKO 2011), and continuous attempts are being made to develop a single universal

* Correspondence: Waldemar Dudda, Katedra Mechaniki i Podstaw Konstrukcji Maszyn, Uniwersytet Warmińsko-Mazurski, ul. Oczapowskiego 11, 10-917 Olsztyn, phone: 48 89/523 32 40, e-mail: waldemar.dudda@uwm.edu.pl

theory. A well designed and executed experiment continues to be the most reliable method of investigating porous media (SOBIESKI, TRYKOZKO 2014a, SOBIESKI, TRYKOZKO 2014b).

This paper is related to a novel research method, described in detail by (SOBIESKI et al. 2012, SOBIESKI, LIPIŃSKI 2014), which relies on a specific combination of microscopic and macroscopic mathematical and physical models for analyzing fluid flow through granular beds. The models are combined with the PathFinder (PathFinder Project 2013, SOBIESKI, LIPIŃSKI 2014) numeric code to calculate a set of geometric parameters of granular beds based on information about the location and diameters of all particles in that bed. Data for calculations in the PathFinder program can be obtained indirectly by developing a virtual bed model with the use of the Discrete Element Method, or directly by generating tomographic scans of the bed sample and analyzing the resulting images. The objective of this study was to describe the new algorithm, whereas the remaining problems have been omitted due to space constraints. The adopted approach could obstruct understanding of the discussed problem, and detailed information about the tortuosity algorithm (SOBIESKI, ZHANG 2012) and the PathFinder program (SOBIESKI, LIPIŃSKI 2014, PathFinder Project 2013) can be found in previous publications.

The previous versions of the PathFinder program (up to version IV.0, inclusive) were developed on the assumption that particles in granular beds are spherical and have constant diameter. In consequence, the triangle defined by centroids of adjacent spheres is roughly equilateral. Therefore, it can be assumed that the center of gravity, S_{gc}, of surface (flow segment) A_p (intersected by the "tortuous flow path") will overlap the center of gravity, S_{tc}, of triangle ABC whose coordinates are defined by the following dependencies (CEWE 2010):

$$\begin{aligned} x_{tc} &= \frac{1}{3}(x_A + x_B + x_C) \\ y_{tc} &= \frac{1}{3}(y_A + y_B + y_C) \\ z_{tc} &= \frac{1}{3}(z_A + z_B + z_C) \end{aligned} \tag{1}$$

where the values in parentheses represent the coordinates of sphere centroids [m] and, consequently, the coordinates of the vertices of triangle ABC.

The determination of the centroid of a triangle composed of three adjacent spheres is a very important consideration in algorithms for calculating the tortuosity of a porous medium (BEAR 1972)

$$\tau = \frac{L_p}{L_0} \tag{2}$$

where: τ – tortuosity [m/m], L_p – ratio of the actual path length inside channels [m], L_0 – thickness of the porous medium [m].

In addition to porosity and specific surface area, the tortuosity of a medium is one of the key parameters characterizing the spatial structure of porous media. In analyses of granular beds, tortuosity is used in the Kozeny-Carman equation (CARMAN 1997, KOZENY 1927, SOBIESKI, ZHANG 2014).

The study proposes a new algorithm for calculating the parameters of granular beds composed of spherical particles with various diameters in the PathFinder program.

Methodology

When spherical particles, including particles with the same radius, are unevenly distributed in a medium, the coordinates of centroid S_{gc} of figure A_p do not match the coordinates of the center of gravity, S_{tc}, of triangle ABC (Fig. 1). The variations in the location of the above points will be even greater when the radii of three spherical particles are different.

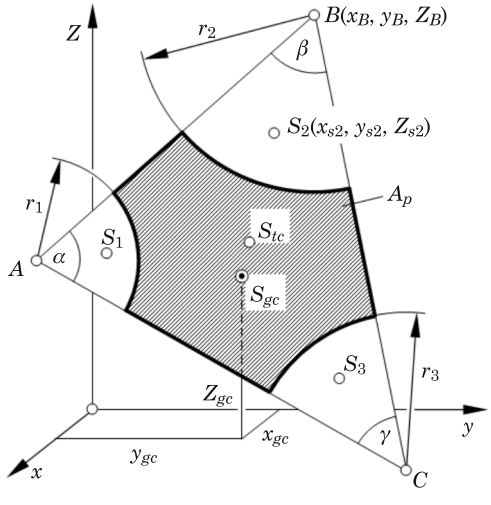

Fig. 1. Surface A_p and its center of gravity, S_{gc}

To solve the problem, a procedure for determining the coordinates of the center of gravity of the shaded region A_p (Fig. 1) has to be developed. The area of the shaded region represents the difference between the area of triangle ABC and the total area of three circular sectors with radii r_1, r_2, r_3 and angles α, β and γ. When the area of each figure and the coordinates of their centers of gravity are known, the coordinates of the center of gravity of surface A_p can be determined with the use of the summation method (LEYKO 2010), which is widely used in mechanics and mathematics:

$$\begin{aligned} x_{gc} &= \frac{A_t\, x_{tc} - A_1\, x_{S1} - A_2\, x_{S2} - A_3\, x_{S3}}{A_t - A_1 - A_2 - A_3} \\ y_{gc} &= \frac{A_t\, y_{tc} - A_1\, y_{S1} - A_2\, y_{S2} - A_3\, y_{S3}}{A_t - A_1 - A_2 - A_3} \\ z_{gc} &= \frac{A_t\, z_{tc} - A_1\, z_{S1} - A_2\, z_{S2} - A_3\, z_{S3}}{A_t - A_1 - A_2 - A_3} \end{aligned} \tag{3}$$

where A_1, A_2 and A_3 represent the area of circular sectors where centers of gravity are located at points $S_1(x_{S1}, y_{S1}, z_{S1})$, $S_2(x_{S2}, y_{S2}, y_{S2})$, $S_3(x_{S3}, y_{S3}, z_{S3})$, respectively.

The area of triangle ABC can be determined using Heron's formula (CEWE 2010):

$$A_t = \sqrt{p(p - AB)(p - BC)(p - CA)} \tag{4}$$

where parameter p, determined by dependence

$$p = \frac{1}{2}(AB + BC + CA) \tag{5}$$

is half that triangle's circumference. The length of the triangle's sides is determined based on the coordinates of the triangle's vertices:

$$\begin{aligned} AB &= \sqrt{(x_A - x_B)^2 + (y_A - y_B)^2 + (z_A - z_B)^2} \\ BC &= \sqrt{(x_B - x_C)^2 + (y_B - y_C)^2 + (z_B - z_C)^2} \\ CA &= \sqrt{(x_C - x_A)^2 + (y_C - y_A)^2 + (z_C - z_A)^2} \end{aligned} \tag{6}$$

The area of circular sectors is defined by geometric dependencies (CEWE 2010):

$$A_1 = \frac{1}{2} r_1 \alpha$$

$$A_2 = \frac{1}{2} r_2 \beta \tag{7}$$

$$A_3 = \frac{1}{2} r_3 \gamma$$

where α, β and γ are vertex angles expressed in radians. Vertex angles are calculated from trigonometric functions when the formulas are transformed to find the area of the triangle (CEWE 2010):

$$\sin \alpha = \frac{2A_t}{AB \cdot AC}$$

$$\sin \beta = \frac{2A_t}{BA \cdot BC} \tag{8}$$

$$\sin \gamma = \frac{2A_t}{CA \cdot CB}$$

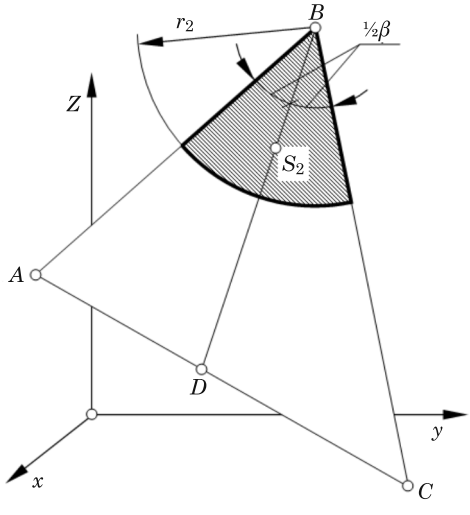

Fig. 2. Location of the center of gravity, S_2, of a circular sector with a centroid at point B

The coordinates of points S_1, S_2 and S_3 have to be calculated to determine the coordinates of point S_{gc} with the use of formula (3). A method for determining coordinates x_{S2}, y_{S2} and z_{S2}, which describe the location of the center of gravity, S_2, of a circular segment with radius r_2 and centroid at point B, is described below. The first step involves the calculation of the coordinates of point D (Fig. 2). Those coordinates are used to determine the bisector of angle β where the center of gravity, S_2, is located. The coordinates of point D are determined based on the coordinates of point A and the coordinates of displacement vector $\overrightarrow{AD}$ based on the following relationship:

$$\begin{bmatrix} x_D \\ y_D \\ z_D \end{bmatrix} = \begin{bmatrix} x_A + x_{AD} \\ y_A + y_{AD} \\ z_A + z_{AD} \end{bmatrix} \tag{9}$$

Segment BD is the bisector of angle β, therefore, the dependence between the lengths of the below segments holds true for triangle ABC:

$$\frac{AD}{AC} = \frac{AB}{CB} \tag{10}$$

When the dependence describing the length of segment AC

$$AC = AD + DC \tag{11}$$

is substituted into equation (10) and when simple transformations are performed, the length of segment AD is expressed as:

$$AD = \frac{AC \cdot AB}{BC + AB} \tag{12}$$

The vector of displacement from point A to point D can be expressed as follows:

$$\overrightarrow{AD} = \overrightarrow{AC^0} \cdot AD = \frac{\overrightarrow{AC}}{AC} \cdot AD = \overrightarrow{AC}\,\frac{AD}{AC} \tag{13}$$

and its coordinates are equal to:

$$\begin{bmatrix} x_{AD} \\ y_{AD} \\ z_{AD} \end{bmatrix} = \begin{bmatrix} x_C - x_A \\ y_C - y_A \\ z_A - z_A \end{bmatrix} \cdot \frac{AD}{AC} \tag{14}$$

Dependence (12) is substituted into formula (14), and the result is substituted into equation (9) to produce formulas for calculating the coordinates of point D:

$$\begin{bmatrix} x_D \\ y_D \\ z_D \end{bmatrix} = \begin{bmatrix} x_A \\ y_A \\ z_A \end{bmatrix} + \begin{bmatrix} x_C - x_A \\ y_C - y_A \\ z_C - z_A \end{bmatrix} \cdot \frac{AB}{BC + AB} \tag{15}$$

The next step involves the determination of the coordinates of point S_2.

The coordinates of point S_2 are calculated based on the coordinates of point B and the coordinates of displacement vector $\overrightarrow{BS_2}$. The searched coordinates are expressed by the following dependence:

$$\begin{bmatrix} x_{S_2} \\ y_{S_2} \\ z_{S_2} \end{bmatrix} = \begin{bmatrix} x_B + x_{BS_2} \\ y_B + y_{BS_2} \\ z_B + z_{BS_2} \end{bmatrix} \tag{16}$$

Centroid S_2 of the circular sector is located on bisector B_D, and its distance from point B (centroid of the circular sector) is defined by the following geometric dependence:

$$BS_2 = \frac{4}{3} r_2 \frac{\sin \frac{1}{2}\beta}{\beta} \tag{17}$$

where vertex angle β is expressed in radians.

The vector of displacement from point B to point S_2 can be expressed as follows:

$$\overrightarrow{BS_2} = \overrightarrow{BD}^0 \cdot BS_2 = \frac{\overrightarrow{BD}}{BD} \cdot BS_2 = \overrightarrow{BD} \frac{BS_2}{BD} \tag{18}$$

therefore, its coordinates are equal to:

$$\begin{bmatrix} x_{BS_2} \\ y_{BS_2} \\ z_{BS_2} \end{bmatrix} = \begin{bmatrix} x_D - x_B \\ y_D - y_B \\ z_D - z_B \end{bmatrix} \cdot \frac{BS_2}{BD} \tag{19}$$

and the length of segment BD is determined based on the following dependence:

$$BD = \sqrt{(x_D - x_B)^2 + (y_D - y_B)^2 + (z_D - z_B)^2} \tag{20}$$

Dependence (17) is substituted into (19) in view of dependence (20). The result is substituted into equation (16) to obtain (after simple transformations) the coordinates of centroid S_2 of the circular sector in the following form:

$$\begin{bmatrix} x_{S_2} \\ y_{S_2} \\ z_{S_2} \end{bmatrix} = \begin{bmatrix} x_B \\ y_B \\ z_B \end{bmatrix} + \begin{bmatrix} x_D - x_B \\ y_D - y_B \\ z_D - z_B \end{bmatrix} \cdot \frac{4r_2 \sin \frac{1}{2}\beta}{3\beta \sqrt{(x_D - x_B)^2 + (y_D - y_B)^2 + (z_D - z_B)^2}} \tag{21}$$

The above process is repeated for circular sectors at points C and A (Fig. 3) to obtain the coordinates of points E and H:

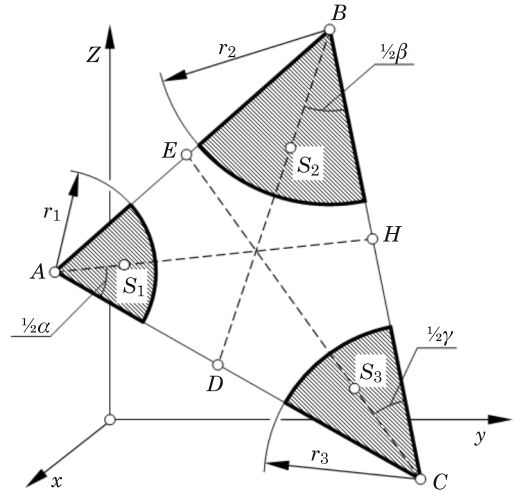

Fig. 3. Location of centroids S_1 and S_3 of the remaining circular sectors

$$\begin{bmatrix} x_E \\ y_E \\ z_E \end{bmatrix} = \begin{bmatrix} x_B \\ y_B \\ z_B \end{bmatrix} + \begin{bmatrix} x_A - x_B \\ y_A - y_B \\ z_A - z_B \end{bmatrix} \cdot \frac{BC}{CA + BC} \tag{22}$$

$$\begin{bmatrix} x_H \\ y_H \\ z_H \end{bmatrix} = \begin{bmatrix} x_C \\ y_C \\ z_C \end{bmatrix} + \begin{bmatrix} x_B - x_C \\ y_B - y_C \\ z_B - z_C \end{bmatrix} \cdot \frac{CA}{AB + CA} \tag{23}$$

and the coordinates of centroids S_3 and S_1, respectively:

$$\begin{bmatrix} x_{S_3} \\ y_{S_3} \\ z_{S_3} \end{bmatrix} = \begin{bmatrix} x_C \\ y_C \\ z_C \end{bmatrix} + \begin{bmatrix} x_E - x_C \\ y_E - y_C \\ z_E - z_C \end{bmatrix} \cdot \frac{4r_3 \sin\frac{1}{2}\gamma}{3\gamma\sqrt{(x_E - x_C)^2 + (y_E - y_C)^2 + (z_E - z_C)^2}} \quad (24)$$

$$\begin{bmatrix} x_{S_1} \\ y_{S_1} \\ z_{S_1} \end{bmatrix} = \begin{bmatrix} x_A \\ y_A \\ z_A \end{bmatrix} + \begin{bmatrix} x_H - x_A \\ y_H - y_A \\ z_H - z_A \end{bmatrix} \cdot \frac{4r_1 \sin\frac{1}{2}\alpha}{3\alpha\sqrt{(x_H - x_A)^2 + (y_H - y_A)^2 + (z_H - z_A)^2}} \quad (25)$$

The coordinates are calculated with the use of formulas (1), (21), (24) and (25), area is calculated based on equations (4) and (7), and the results are substituted into formula (3) to obtain the coordinates of the center of gravity of figure A_p.

The parameters of figure A_p, which are applied in the computational program, include its area:

$$A_F = A_t - A_1 - A_2 - A_3 \quad (26)$$

and circumference:

$$p_F = 2(p - r_1 - r_2 - r_3) + (\alpha \cdot r_1 + \beta \cdot r_2 + \gamma \cdot r_3) \quad (27)$$

where angles α, β and γ are expressed in radians.

Validation of derived dependencies

The presented algorithm was used to develop a numeric procedure in the Fortran 90 programming language. The subprogram calculates the coordinates of the centroid of figure A_p based on the input coordinates of triangle vertices and the radii of circular sectors. The procedure was implemented in the PathFinder program to determine the tortuous flow path. In the main program, the positions of three spherical particles are used to calculate the position of the fourth particle making up the tetrahedron. The position of the fourth spherical particle is calculated by determining the normal to the triangle surface intersecting the center of gravity of figure A_p. In a numerical

analysis of a bed comprising thousands of spherical particles, the position of adjacent tetrahedrons, which form the region of the tortuous flow path, is determined. The path is mapped by combining the centroids of figures A_p of adjacent tetrahedron sides. Path length is the total length of the segments combining the centroids of successive figures A_p in the region of the entire tortuous flow path. The procedure of determining the coordinates of a centroid of the current surface A_p is called before the search for every successive tetrahedron is initiated in accordance with the discussed algorithm.

The coordinate calculation procedure was verified in the AutoCAD program. The coordinates of any graphically represented flat or solid figure can be determined in the AutoCAD environment independently of the applied algorithm. The validation process was performed for a triangle with vertex coordinates $A(10,3,4)$, $B(2,20,30)$ and $C(20,30,10)$, from which circular sectors with radii R of 5, 6 and 8, respectively, had been removed (Fig. 4). The resulting figure, represented by the shaded region in Figure 4, was created with the use of an AutoCAD command. The physical properties of that region were determined in the program. A text window with the parameters of the selected region, including area, circumference and centroid coordinates, is presented in Figure 5.

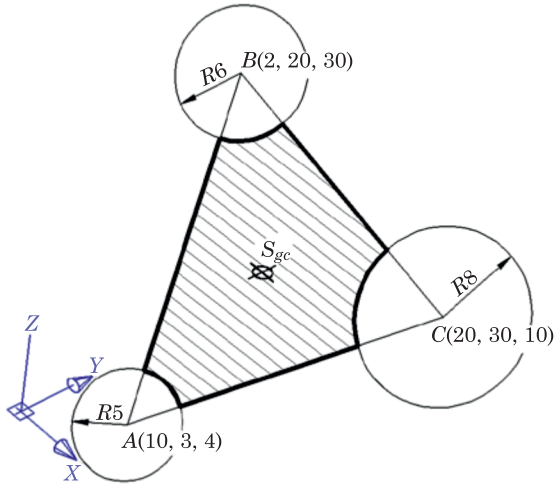

Fig. 4. Surface A_p determined in the AutoCAD program

Figure coordinates were calculated in the subprogram written in Fortran based on the dependencies derived in Chapter 2. The results are presented in Table 1. The results produced by the discussed algorithm (Table 1) and the results generated in AutoCAD are identical (Fig. 5). The derived dependencies and the numerical subprogram were thus positively validated.

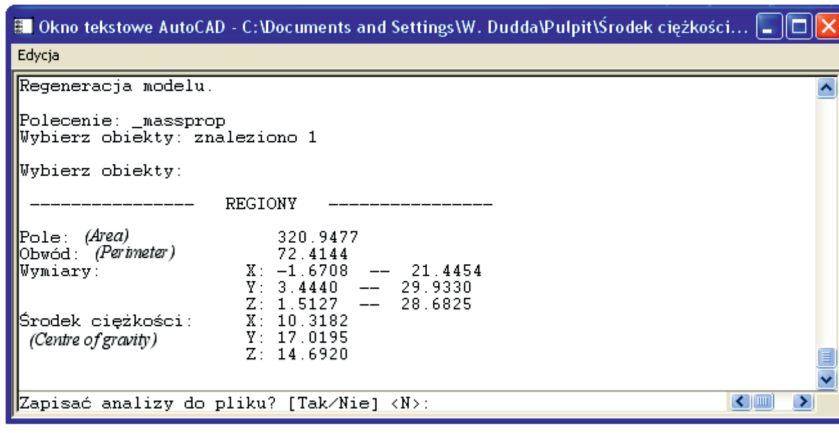

Fig. 5. Centroid coordinates determined in the AutoCAD program

Table 1

The results of geometric calculations

Coordinates of triangle centroid (x_{tc}, y_{tc}, z_{tc})	Angles (α, β, γ)	Area of circular sectors (A_1, A_2, A_3)	Coordinates of circular sector centroids [m]			Coordinates of the center of gravity (x_{gc}, y_{gc}, z_{gc})	Figure area (A_F)	Figure circumference (p_F)
			S_1 (x_1, y_1, z_1)	S_2 (x_2, y_2, z_2)	S_3 (x_3, y_3, z_3)			
[m]	[°]	[m^2]	[m]	[m]	[m]	[m]	[m^2]	[m]
10.6667	55.4537	12.0981	10.1640	3.9169	17.0806	10.31816		
17.6667	57.5555	18.0816	5.6212	19.6028	26.1772	17.01952	320.9477	72.4144
14.6667	66.9908	37.4147	5.8365	26.7035	11.4874	14.69201		

Comparison of tortuous flow paths (previous and new version)

The effect of changes in the computational algorithm on program performance was verified by performing comparative calculations in a granular bed generated by the Discrete Element Method in PFC^{3D} (LIU et al. 2008a, LIU et al. 2008b). Bed parameters and basic PathFinder settings (refer to the User's Guide (SOBIESKI, LIPIŃSKI 2014)) are presented in Table 2.

The results of both computational methods and a model ISP (in this case: a centroid) are presented in Table 3. As expected, a change in the algorithm modified the course of the path in space, including its total length, average angles between segments and tortuosity. The remaining parameters remained unchanged.

The changes in point positions were relatively small, but they significantly influenced the course of different paths. The above is illustrated by Figure 6

Table 2

Basic parameters of the flow set

Parameter	Value
Domain geometry	cylinder
Number of particles	18188 [–]
Particle diameters	5.5–7.5 [mm]
Average diameter	6.45 [mm]
Number of particles rejected from the top surface	19 [–]
Method for calculating the triangle centroid	triangle centroid / center of gravity
Characteristic dimension	l_{ave} [m]
Correction method for the Ideal Location	function
Correction based on the critical area of the triangle	yes
Critical normalized area of the triangle	3.0 [–]

where paths momentarily follow the same flow channels, then change direction and become completely separated. In some cases, previously separated paths are repeatedly merged. Even if paths follow the same flow channels, they do not overlap. Changes in three model paths for ISP = '00' (the results for this path are presented in Table 3), ISP = '– –' and ISP = '++' are presented in Figure 6. Symbols '–', '0' and '+' denote the location of the ISP relative to the centroid of the surface that constitutes the bottom wall of the bin (SOBIESKI, LIPIŃSKI 2014).

Table 3

Comparison of results

Parameter	Triangle centroid	Centre of gravity	Unit
Initial Staring Point	00		[–]
xshift / yshift	0.5 / 0.5		[–]
Number of path points	129	130	[–]
Number of path rejected points	1	0	[–]
Number of corrected triangles	0	0	[–]
Bed height	0.254938		[m]
Path length	0.315499	0.317288	[m]
Average angle between path sections	137.859292	140.183486	[°]
Tortuosity	1.237553	1.244571	[m/m]
Tortuosity determined by the formula of Yu and Li	1.632555		[m/m]
Bed volume (bulk volume)	0.004505		[m^3]
Inner surface of the solid body	2.393343		[m^2]
Specific surface of the porous body (K)	531.227627		[1/m]
Specific surface of the porous body (C)	915.918417		[1/m]
Volume of the porous body	0.002613		[m^3]
Porosity	0.420006		[m^3/m^3]

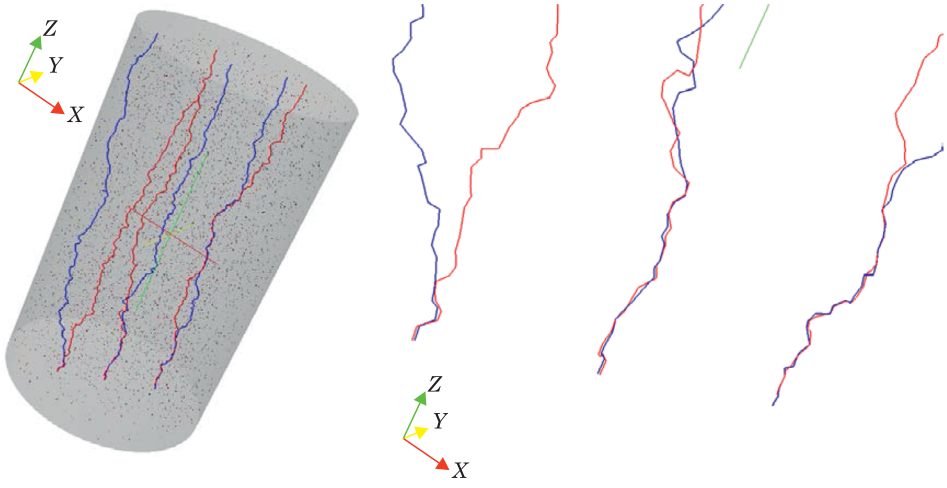

Fig. 6. Paths determined with the use of different methods: triangle centroid (blue) and center of gravity (red)

The values of the quality indicator for predicting the location of tetrahedron vertices (an important part of the algorithm for tortuosity evaluation – refer to (SOBIESKI, ZHANG 2014) are presented in Figure 7. The lower the value of the quality indicator, the greater the algorithm's efficiency in predicting the location of successive spheres surrounding the path (spheres divided by the path). The data presented in Figure 7 indicates that an algorithm based on centers of gravity often produces more satisfactory results.

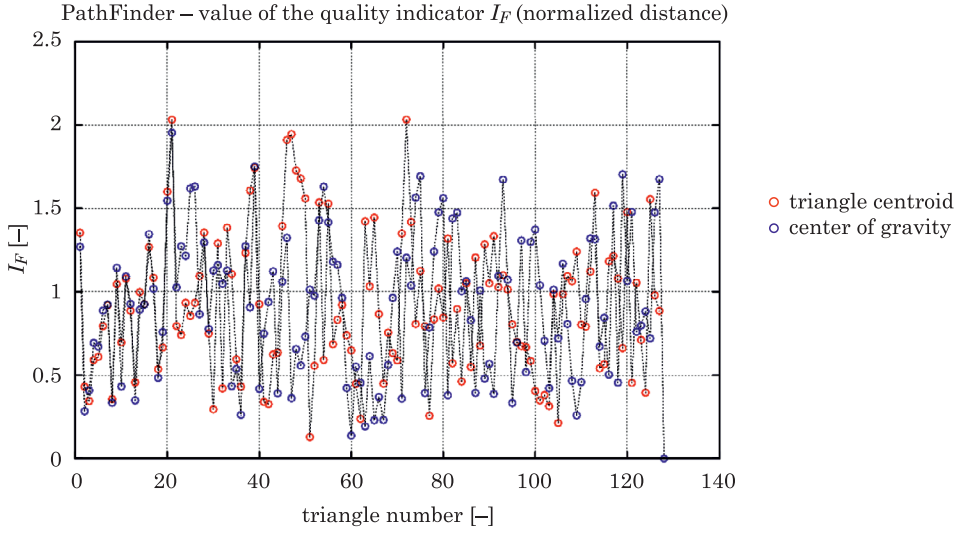

Fig. 7. Values of the quality indicator for predicting the location of tetrahedron vertices

Conclusions

The following conclusions can be formulated based on the results of the study:

– A universal algorithm was developed for calculating the center of gravity of a figure intersected by a flow path. The algorithm was verified with the use of independent computational tools (AutoCAD program) and successfully implemented in the source code of the PathFinder program.

– The new version of the computational algorithm influences only the length of the flow path, the angles between path segments and path tortuosity. The remaining parameters and indicators remain unchanged.

– The new algorithm is more logically justified, and it increases the quality of predicting the location of successive spheres. For this reason, it will be recommended as the default algorithm in the upcoming versions of the PathFinder program, beginning from version IV.1.

References

BEAR J. 1972. *Dynamics of Fluids in Porous Media*. Dover, New York.

CARMAN P.C. 1997. *Fluid Flow through a Granular Bed. Transactions of the Institute of Chemical Engineers*. Jubilee Supplement, 75: 32–48.

CEWE A., NAHORSKA H., PANCER I. 2010. *Tablice matematyczne*. Wydawnictwo Podkowa, Warszawa, p. 1-143.

KOZENY J. 1927. *Über kapillare Leitung des Wassers im Boden*. Akademie der Wissenschaften in Wien, Sitzungsberichte, 136(2a): 271–306 (in German).

LEYKO J. 2010. *Mechanika ogólna*. PWN, Warszawa. Tom 1. p. 1–392.

LIU C., ZHANG Q., CHEN Y. 2008a. *PFC^{3D} simulations of lateral pressures in model bins*. Paper No 083340, American Society of Agricultural and Biological Engineers, St. Joseph, MI.

LIU C., ZHANG Q., CHEN Y. 2008b. *PFC^{3D} simulations of vibration characteristics of bulk solids in storage bins*. Paper No 083339, American Society of Agricultural and Biological Engineers, St. Joseph, MI.

PathFinder Project 2013. On-line, http://www.uwm.edu.pl/pathfinder/index.php (available at February 7, 2014). University of Warmia and Mazury in Olsztyn.

SOBIESKI W., LIPIŃSKI S. 2014. *PathFinder User's Guide*. On-line: http://www.uwm.edu.pl/pathfinder/index.php (available at 7 February 2014). University of Warmia and Mazury in Olsztyn.

SOBIESKI W., TRYKOZKO A. 2014a. *Darcy's and Forchheimer's laws in practice*. Part 1. *The experiment*. Technical Sciences (submitted).

SOBIESKI W., TRYKOZKO A. 2014b. *Darcy's and Forchheimer's laws in practice*. Part 2. *The numerical model*. Technical Sciences (submitted).

SOBIESKI W., TRYKOZKO A. 2011. *Sensitivity aspects of Forchheimer's approximation*. Transport in Porous Media, 89(2): 155–164.

SOBIESKI W., ZHANG Q., LIU C. 2012. *Predicting Tortuosity for Airflow through Porous Beds Consisting of Randomly Packed Spherical Particles*. Transport in Porous Media, 93(3): 431–451.

SOBIESKI W., ZHANG Q. 2014. *Sensitivity analysis of Kozeny-Carman and Ergun equations*. Technical Sciences (in press).